Composites Communications 45 (2024) 101797

Contents lists available at ScienceDirect

Composites Communications

journal homepage: www.elsevier.com/locate/coco

Short Communication

Influence of mold pressurization on cycle time in rotational molding composites with welded ignimbrite as loading

Zaida Ortega [a,*], Paula Douglas [b], Paul R. Hanna [b], Jake Kelly-Walley [c,d], Mark McCourt [b]

[a] Departamento de Ingeniería de Procesos, Universidad de Las Palmas de Gran Canaria, Edificio de Ingenierías, Campus Universitario de Tafira Baja, 35017, Las Palmas, Spain
[b] Polymer Processing Research Centre, Queen's University of Belfast, Belfast, BT9 5AH, Northern Ireland, United Kingdom
[c] School of Mechanical and Aerospace Engineering, Queen's University of Belfast, Belfast, BT9 5AH, Northern Ireland, United Kingdom
[d] Matrix Polymers, Unit 2, Compass Industrial Park, Spindus Road, Speke, Liverpool, L24 1YA, United Kingdom

ARTICLE INFO

Keywords:
Rotomolding
Cycle time reduction
Pressure
Energy consumption
Ignimbrite
Mineral dust
Waste valorization
Composite

ABSTRACT

In the context of rising energy costs and climate emergencies, there is a need to incorporate novel procedures or materials to meet sustainability requirements and increase the efficiency of processes and use of resources. Although rotational molding might seem disadvantageous due to the long cycle times and high energy consumption, its inherent advantages, including the production of hollow parts of any size without wasting materials, with good surface reproducibility and no internal stresses, using cost-effective tooling remain noteworthy. To address energy consumption concerns, increase productivity, and enhance the environmental footprint of rotomolded products, this work proposes the incorporation of residual welded ignimbrite from quarries, a dusty material with over 60 % of SiO_2, combined with the mold pressurization, finding a 4 % reduction of total cycle time with ignimbrite, which is further shortened to 12 % when pressure is applied. Particularly notable is the reduction 27 % reduction in oven time when using ignimbrite at 10 % under pressure. The thermomechanical and rheological characterizations revealno adverse effects either by the use of pressure or the mineral dust, thus establishing a viable alternative for energy (and cost) reduction. Besides, the obtained parts show good aesthetics, a stone-like aspect, which might provide additional features for applications such as outdoor furniture or storage tanks.

1. Introduction

Rotomolding allows the obtaining of hollow parts with null or low internal stress, no welding lines, low-cost molds, and minimal waste [1,2]. This sector is forecasted to grow at a rate of about 6 % yearly, reaching 8500 million euros by 2031 [3]. Some aspects hindering a broader expansion of the technology are the long cycle times needed together with the narrow range of available materials [2], dominated by polyethylene (PE) in powder form [2], due to its low viscosity and good thermal stability [4]. The rotomolding process consists of different steps, simplified into material loading into the mold, rotomolding, cooling, and part demolding. The mold is under rotation during the rotomolding and cooling stages, usually over two axes [5,6]. During the rotomolding step itself, three main phenomena are observed, based on the internal air temperature (IAT) monitoring; these stages are [5,7,8]:

i) Increase in the IAT and the polymer material: induction.
ii) Unchanged temperature at melting temperature: sintering, the material starts melting and sticking in the mold walls.
iii) Fast increase in IAT: densification, the air bubbles trapped in the bulk migrate towards the inside of the mold and escape through the vent. The maximum temperature reached is the peak internal temperature (PIAT).

Different strategies can be followed to increase the sustainable character of rotomolded parts and overcome their main limitations, from using bio-based [9–13] or recycled [14–18] materials, either as polymer or as a filler, to the use of novel tooling. In this sense, some authors have worked on induction, electrical or microwave-heated tools [19,20], microwave-assisted processes or optimized molds with improved heat efficiency obtained by combining two different metals: nickel for hardness and copper for thermal conductivity [21]. The use of

* Corresponding author.
E-mail address: zaida.ortega@ulpgc.es (Z. Ortega).

https://doi.org/10.1016/j.coco.2023.101797
Received 21 October 2023; Received in revised form 14 December 2023; Accepted 18 December 2023
Available online 20 December 2023
2452-2139/© 2023 The Authors. Published by Elsevier Ltd. This is an open access article under the CC BY license (http://creativecommons.org/licenses/by/4.0/).

directly heated molds, using a Robomould device [19], results in lower energy consumption (up to 15 times less than in conventional carrousel machines), higher energy efficiency, and shorter cycle time (about 20 %) due to the reduced time needed to heat the mold. Internal pressurization is a different strategy to reduce cycle time and improve final parts properties (such as reduced shrinkage or increased ductility). In this sense, only one reference has been found; Malnati [22] reported cycle times reductions of up to 78 % for 6.35 mm thick parts made on PE when using pressure-assisted cooling by ' 'Ripple's technology. However, this author only provides the data; neither the curves nor the properties of the obtained parts have been found in the literature.

Lignocellulose fillers have been incorporated into rotomolded products as a way to improve the features of the obtained products, including the environmental footprint [23], particularly when using wastes or by-products, such as in the case of banana fibers [24], wood dust [25], wheat bran [26], or buckwheat husks [12]. These materials are introduced at ratios not usually over 10 % in weight to avoid the excessive presence of voids and the deterioration of the mechanical properties. The incorporation of such materials, which are known to provide thermal insulation, usually results in cycle time increases [27], particularly due to the delayed reaching of PIAT because of an extended induction step; a positive trend is found between the ratio of fiber and the cycle time, getting increases of 8, 10 and 18 % for 5, 10 and 20 % abaca/PE composites, respectively [13]. [28] Despite their attractive thermal stability, less work has been done on the incorporation of inorganic fillers in rotomolding [28]. Some authors have proposed the use of quartz [29] or clay [30,31]; very limited research is available on the use of inorganic residual materials, such as copper slag [18]. Other materials, such as basalt or marble dust, as residues from stone production, have not yet been explored in the literature for rotational molding. There is also very limited research on their use in other polymer processing technologies, mainly on injection molding [32–37]. This work proposes the use of ignimbrite dust, a residue from high-quality stone products in the Canary Islands (Spain), as a loading for rotomolded products; during the different operations performed on the stone, a high volume of residues, currently without any use, is produced. This stone is of great ethnographic and economic value and shows a high content in silica (62.5 %) and alumina (17.8 %), with lower values of Na_2O (6.4 %), K_2O (4.7 %) and FeO/Fe_2O_3 (3.6 %) [38]. As this consists of fine dust, it is used without further modifications and introduced in the process by simple dry-blending.

Therefore, this work aims to determine how mold pressurization (0.8 bar) and the incorporation of a mineral loading affect the rotomolding cycle time for obtaining standard cube-shaped 4-mm thick PE parts. The thermomechanical properties of the obtained parts have been assessed as a way to demonstrate the use of pressure or the incorporation of the mineral dust is not negatively affecting the rotomolded samples, thus constituting a suitable strategy to reduce their environmental footprint without performing any complicated modifications in conventional rotomolding apparatus. This research responds to the needs of the rotomolding sector to advance towards a more sustainable process, by the valorization of a residual material and the shortening of cycle-times (and energy consumption).

2. Materials and methods

2.1. Materials

The material used was a polyethylene-hexene grade from Matrix Polymers (Revolve N-307), with a density of 0.939 g/cm^3 and a melt flow index of 3.5 g/10 min. The ignimbrite dust was supplied by Compañía Artesanal de Cantería de Arucas S.L. (density of 2.45 g/cm^3 and particle size between 6 and 50 μm) and was used without any modification.

2.2. Rotational molding trials

Samples were produced in a 200 × 200 × 200 mm aluminum mold with a vent hole in a biaxial three–arm carrousel rotomolding machine from Ferry RotoSpeed, RS–1600 Turret Style model. The rotational speed ratio was set to 8:2, and the oven temperature was set at 300 °C. The oven and peak internal air temperature (PIAT) were constantly monitored using a Rotolog system. For those parts with positive internal pressure applied, the vent was substituted by a pipe with a valve, which was opened for gas outlet during the first stages of heating and closed for air injection when the sintering stage concluded, that is, the valve is open (ambient pressure) during the first stages of the molding (heating and sintering) and closed (increased pressure) for densification and cooling.

Samples without pressure application were heated until reaching an IAT of 180 °C; for those with pressure, the mold was taken out of the oven at 140 °C, at a pressure of 0.8 bar. The cooling was performed with forced air until it reached 70 °C when parts were extracted from the mold. The total weight of material in each sample was 800 g, which allowed obtaining 4 mm-thick parts.

The composites were prepared by dry-blending the polymer and the mineral powder in different proportions, ranging from 5 to 20 wt %.

2.3. Rotomolded items characterization

The flow properties of the materials were assessed in an oscillatory rheometer AR G2 from TA Instruments, with 25 mm diameter parallel plates and a 1.5 mm gap under a nitrogen atmosphere. The experiments were conducted at 190 °C. Preliminary assays were performed under the strain sweep mode in order to ensure later experiments were placed in the linear viscoelastic region (LVR). In these tests, the strain was varied between 0.1 and 5 %. Frequency sweep tests were performed at 0.5 % strain, in the LVR, in the 100 to 0.01 Hz range. Finally, flow tests were also performed at the same temperature, between 0.01 and 1 Hz shear rate.

The thermomechanical properties of the different materials were evaluated by Dynamic Mechanical Thermal Analysis (DMTA) using a Tritec 2000 device from Triton Technology under the single cantilever bending method. A strain of 10 μm was applied at 1 Hz frequency between −60 and 100 °C, with a heating rate of 2 °C/min.

3. Results and discussion

3.1. Rotomolded items aspect and dust distribution

Fig. 1 shows the aspect of the items obtained. Samples with 5 and 10 % in weight of the mineral dust were successfully rotomolded, bringing parts with good aspect, low voids either in the external surface or the wall thickness, and good dust distribution. However, those moldings with higher filler ratios (20 %) were not adequately molded (Fig. 1a). As observed below, the material could not form entirely during the molding; this might be due to the abrasion of the mineral dust, which, during the rotation, peeled off the layer of molten polyethylene from the mold walls. As usually observed in other research works, loadings over 10 % are not recommended; using melt-compounding might help increase the amount of loading.

Nevertheless, parts with up to 10 % show a good distribution of the dust within the matrix (Fig. 1b). Once the dust is integrated within the matrix, this abrasion is expected to be reduced. It is observed that good aesthetics, a stone-like aspect, is obtained, with a darker color when the loading of mineral filler increases. The use of pressure does not modify the aspect of the parts, but is only helpful in reducing the warpage, particularly for neat PE samples.

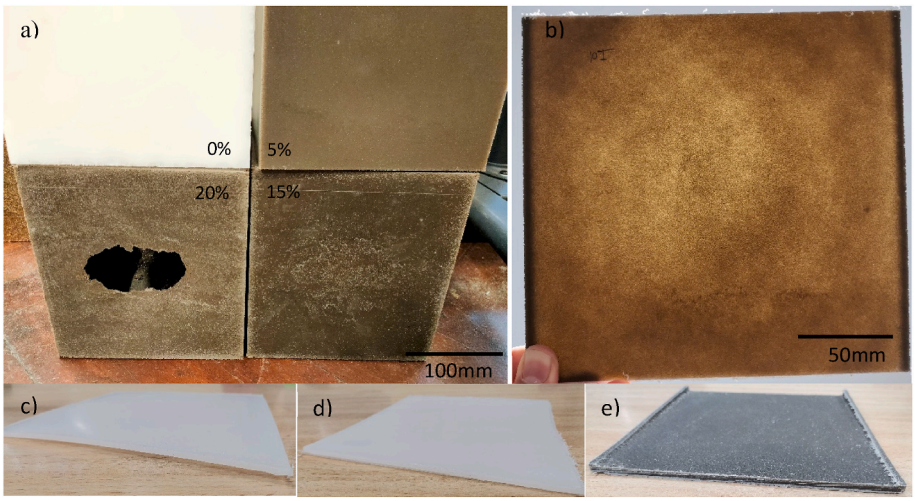

Fig. 1. Photographies of rotomolded products: a) cubic molds at 0, 5, 15, and 20 % loadings, b) distribution of dust in a side of the cube for 10 % mineral dust, c) one side of the cube for PE sample, showing warpage, d) one side of the cube for PE sample rotomolded with pressure, with no warpage, e) one side of the cube at 10 % loading with pressure.

3.2. Cycle time analysis

Fig. 2 shows the cycles recorded for the PE rotomolding trials. The reduction in oven time can be observed in Fig. 2a, with data analyzed in Table 1. As observed in Fig. 2b, the different stages are clearly identified, i.e. heating, sintering, densification and cooling. As indicated in the methods section, the PIAT for moldings under pressure was reduced, finding parts well-consolidated and with good properties, not achievable without the use of pressure. Nevertheless, a sample of neat PE was produced at the same temperature, with and without pressure, to check the properties of the rotomolded sample, finding no differences between them, nor with the sample processed at a lower temperature. It was then established that such temperature reduction does not result in lowered consistency or properties of the rotomolded items. Therefore, cooking the parts at that temperature value is possible, which relates to a significant reduction in time and energy.

As said, the use of pressure is necessary if this lower temperature is to be used; otherwise, the resulting parts will not be well-formed. This is due to the fact that the pressure pushes the polymer through the mold walls, achieving a more effective transfer of heat between mold and bulk material, as the PIAT is not so different from the moldings without pressure to the pressurized ones. For instance, the PIAT for non-pressurized PE moldings was 206 °C, while for pressurized mold it arrived at 190 °C, despite taking the sample out of the oven at 180 vs. 140 °C. A similar trend is observed for the composite samples (Table 1).

Apart from this, the reductions in oven time are observed, arriving at up to a 27 % decrease, as found in Table 1. The decreased overall cycle time is also evident from Fig. 2b, where faster heating (induction, sintering, and densification) is found for composites with 10 % loading. The time elapse until reaching PIAT is about 11.7 min for 10 % composites, which constitutes a shortening of about 10 % in this stage compared to neat PE, regardless of the use of pressure, while only using pressure on neat PE also reaches similar time reductions. This, which is the result of a shorter densification stage (from 4.3 to 4.7 min for moldings with no applied pressure to 2.4 min for pressurized PE and 3.6 min for 10I-P), might be due to the enhanced heat transfer because of the pressure and the higher contact between polymer and mold, as already mentioned. Induction and sintering steps are not affected, as the pressure is applied once sintering has ended; however, faster induction and sintering are observed for the composites as a consequence of the lower heat capacity of the mineral (1550 J/kgK for PE vs. 800 J/kgK for ignimbrites [39]). On the other hand, the cooling cycle is affected mainly by the use of pressure, with the incorporation of minerals not significantly affecting the overall cooling.

Therefore, it seems that both the incorporation of the mineral dust and the mold pressurization results in rotomolding cycle time

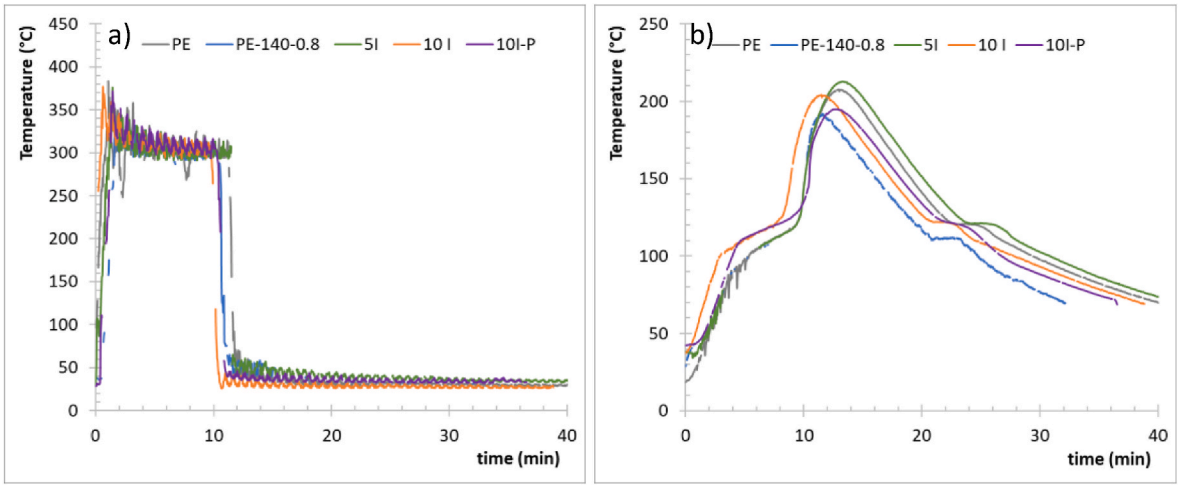

Fig. 2. a) Temperature recordings for the thermocouple placed outside the mold, b) Monitoring of internal air temperature.

Table 1
Distribution of time for each stage of the rotomolding cycle and variations compared to the PE molding cycle without any pressure applied.

Cycle	Oven time		Cooling time		Total cycle time		PIAT	Time to reach PIAT	
	(min)	Variation (%)	(min)	Variation (%)	(min)	Variation (%)	(°C)	(min)	Variation (%)
PE	11.9	–	27.6	–	40.3	–	207.3	13.2	–
PE-P	10.6	−11 %	20.7	−25 %	32.3	−20 %	190.2	11.6	−12 %
5I	11.4	−4%	26.5	−4%	39.7	−2%	211.3	13.1	0 %
10I	9.8	−17 %	27.0	−2%	38.8	−4%	203.6	11.7	−11 %
10I-P	8.8	−27 %	23.5	−15 %	35.5	−12 %	194.8	12.0	−9%

reductions, making the pressure a more significant factor than the mineral loading. Not only is the total time reduced but also the oven time, which is linked to energy consumption and productivity.

3.3. Rheology assessment of rotomolded samples

The rheological behavior of the materials plays an essential role in rotomolding, as high viscosity would hinder an appropriate flow of the material inside the mold and impede the migration of air bubbles in the densification step [4,7]. As observed in Fig. 3, no differences in the rheological behavior of the PE are found as a consequence of the incorporation of air pressure during molding in the entire range of frequencies studied. This constitutes proof that no bulk material modifications (such as oxidation or cross-linking) are happening in the process [23], regardless of the application of pressure. A similar observation arises for the composites (Fig. 3a), with no significant alterations on storage or loss modules; only storage modulus is slightly increased for composites loaded at 10 %, while loss modulus remains overlapped for all materials. This is translated in all the materials showing similar viscoelastic behavior, with a well-defined Newtonian plateau, and similar viscosity values along the entire range of shear rates studied (Fig. 3b), with all samples exhibiting a certain shear thinning behavior at high shear rates. This means that neither the application of pressure nor the incorporation of up to 10 % of the ignimbrite dust affects the polymer flow properties, which is in accordance with the excellent moldability. Generally, the incorporation of fillers results in increased viscosity, or lowered melt flow index [18,23], while some fillers (basalt dust) have shown a behavior close to that reported here [40], that is, no effect on the viscous behavior of the matrix. The good dispersion of the filler is also evidenced by drawing the Cole-Cole plot (Fig. 3c), which is a comparison between the real and imaginary parts of viscosity. The closer the shape obtained to a circle, the higher the homogeneity of the blend [41,42]. It can be observed that the curves for ignimbrite composites are close to a semicircle and, again, are almost overlapped with those for neat PE; in any case, the curves at 10 % loading show some deviation from the PE ones, showing that this is probably the limit of loading to be used without interfering in the viscose properties during the processing. The pressure does not seem to have any impact on the polymer's rheological behavior. Zero-shear viscosity values (η_0) also show similar behavior for each material, regardless of the use of pressure, i.e., approximately 2300 Pa s for PE and 5 % composites, and about 5000 Pa s for 10 %.

The similarities in the rheological behavior between the different series, despite the incorporation of the ignimbrite dust, are in line with the excellent quality of the parts obtained; that is, the introduction of the fillers does not negatively affect the flow behavior of the polymer inside the mold, allowing to obtain parts with good aesthetics and properties, and without evident voids or bubbles in the bulk material neither in their inner or outer surfaces.

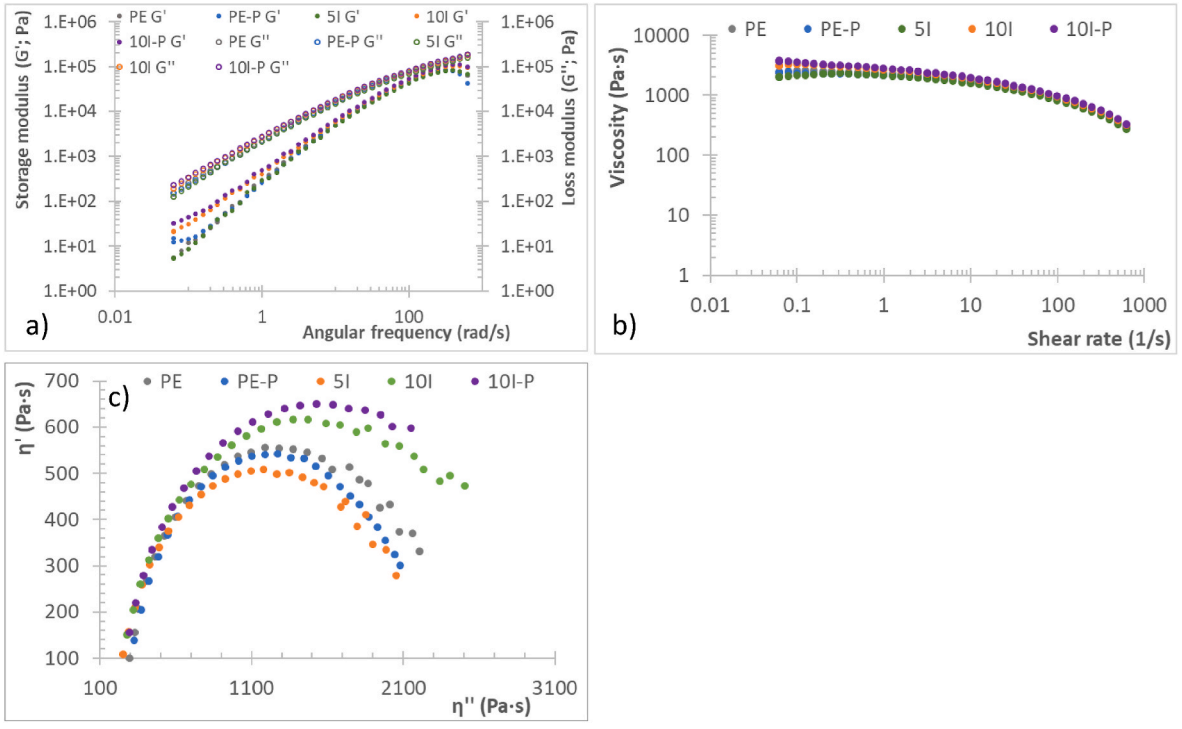

Fig. 3. Rheological behavior of PE rotomolded samples: a) storage (left) and loss (right) modulus versus angular frequency, b) viscosity versus shear rate, c) Cole-Cole plot.

3.4. Thermomechanical performance of rotomolded samples

The analysis of storage modulus (E′), loss modulus (E"), and damping factor (tan δ) obtained from Dynamic Mechanical Analysis (DMA) allows evaluating the change of mechanical properties in the temperature range studied (−60 to 100 °C) [43]. The curves for the different moldings follow the expected course (Fig. 4a), with a decreasing trend with temperature. No significant differences are observed for polyethylene samples due to the mold pressurization (curves for PE and PE-P are completely overlapped). The incorporation of ignimbrite in 5 % increases the storage modulus, particularly at low temperatures, meaning the filler is stiffening the matrix; however, for 10 % loadings, this effect tends to disappear, showing a reduction in storage modulus in the temperature range studied, which is reduced as temperature increases. The literature reflects that storage modulus from DMA analysis are correlated with the values of elastic modulus from statice tensile tests [31]; therefore, as the values of E' are not reduced because of the incorporation of the ignimbrite dust, it is expected that the obtained composites would exhibit a performance under tensile testing similar to that of PE. Interestingly, the use of pressure in the composite increases E', which again reaches values close to neat PE. It then seems that mold pressurization for composites obtaining, without any melt-mixing process, might result in better integration of the filler within the matrix.

Regarding the damping factor (in dashed lines in Fig. 4), it can be seen that the curves follow a similar trend. Finally, for the loss modulus, the curves are mostly overlapped, observing two maximums in the curve, one at approximately −20 °C, which can be related to segmental motions in the amorphous region [44], and a more intense one at 44–47 °C, attributed to α-transition (chain movements in the crystalline region) [26]. These same conclusions arise from the damping factor curves, as also reported in previous research works [31]. Therefore, the similarities in the viscous behavior, observed as a similar damping factor, is a confirmation of the lack of modification in the polymer bulk.

From the DMA results, the adhesion factor (A) can be obtained, as described by Kubát et al. [45], who consider that the behavior of the composite is due to the properties of the matrix, the filler and the interphase (equation (1)):

$$A = \frac{1}{1 - x_F} \cdot \frac{tan\ \delta_C}{tan\ \delta_{PE}} - 1 \quad (1)$$

Where x_F is the ratio of the filler in the composite (in volume), and tan δ_C and tan δ_{PE} are the damping factors of the composite and the neat PE, respectively.

The entanglement factor (N) is also proposed as an approximation to the intensity of the interaction between matrix and filler/reinforcement, together with the efficiency factor [46,47]. The entanglement factor is usually calculated at several temperatures to evaluate the potential differences in such interactions due to different service conditions; in this manuscript, the variation of this factor with temperature is shown in Fig. 4c and is calculated as:

$$N = \frac{E'}{RT} \quad (2)$$

Where E' is the storage modulus at a specific temperature (T, in K) and R is the universal gas constant.

The reinforcement efficiency (r), calculated as shown in equation (3), provides information about the filler/matrix interaction:

$$E'_c = E'_m \cdot (1 + r \cdot V_f) \quad (3)$$

Where E'_c and E'_m are the storage modulus of the composite and the matrix, respectively, and V_f is the percentage of the filler (by volume).

Lower values of A indicate higher interfacial adhesion, which should correlate with a higher mechanical behavior [26]. As this factor depends on the damping factor, it also varies with temperature (Fig. 4b). It can be seen that 10 % composite exhibits the highest value of the adhesion factor, which means it shows a lower compatibility or higher porosity [26]; on the opposite, both 5I and 10I-P show an adhesion factor close to zero, lower even for 10I-P, showing the beneficial effects of pressure for the obtaining of particulate composites. Similarly, the entanglement factor is reduced for 10I, also showing it is acting as a filler and reducing the mechanical behavior of the PE (r < 0); the reinforcement efficiency

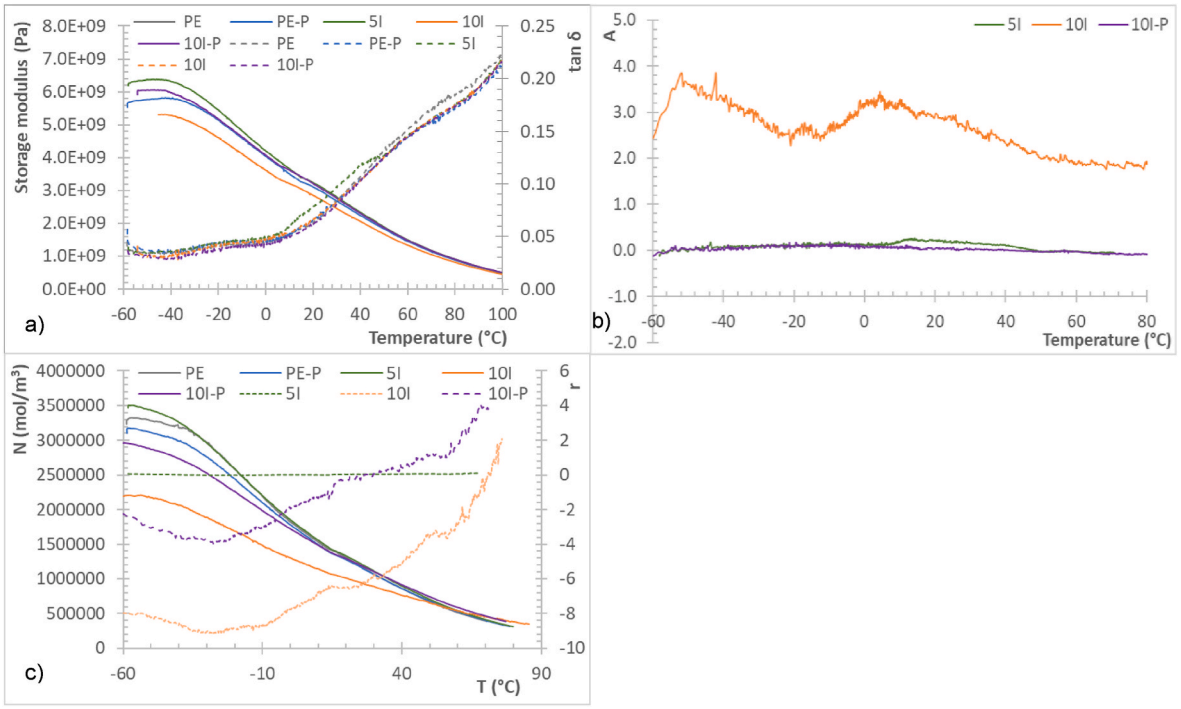

Fig. 4. a) Variation of storage modulus (line, left axis) and damping factor (dashed line, right axis) for the rotomolded samples, b) Adhesion factor for the ignimbrite/PE composites, c) Entanglement factor (solid lines, left axis) and reinforcement efficiency (dashed lines, right axis).

for 5 % composites is almost zero in the entire range of temperature studied, meaning it is not affecting the mechanical behavior of the matrix, while 10I-P seems negatively affecting the behavior of PE at low temperatures and effectively reinforcing it at temperatures over 20 °C.

4. Conclusions

The mold pressurization during the densification and cooling stages yields a significant reduction in rotomolding cycle time. Particularly, reductions in oven time over 10 % are achievable for neat polyethylene, with potential reductions of up to 27 % when also introducing a 10 % weight of the ignimbrite dust. An overall cycle time reduction of up to 20 % results from the increased cooling rate due to pressure use.

The polyethylene's rheological behavior remains unaffectedis not affected by the use of pressure or the introduction of mineral dust, indicating no significant alternations in the polymer bulk. Consequently, polymer oxidation due toair incorporation does not occur in the process. Furthermore, mold pressurization lowers the temperature at which the mold is removed from the oven, thus being an advantage for thermosensitive polymers by requiring lower heating times and temperatures obtain well-consolidated parts. Besides, shifting air to any other inert gas would prevent any further oxidation or degradation reactions.

Finally, using pressure enhances thermomechanical behavior of 10 % composites, yielding a near-zero adhesion factor close in the temperature range studied and even showing a reinforcing effect at temperatures over 20 °C. In contrast, the composites with 5 % filler show no difference from neat PE.

Incorporating a mineral dust material, widely available at no or low-cost, is an effective strategy to reduce cycle time while providing parts stone-like parts with good aesthetics and thermomechanical stability, particularly when obtained under pressure. Further studies are needed to assess these strategies' impact on the behavior of rotomolded products, such as moisture uptake, durability, or insulation characteristics. Besides, the technical feasibility of mold pressurization, particularly for large-sized products, requires further analysis, including a cost analysis. A comprehensive life cycle assessment considering the partial substitution of the polymer by industrial waste, the energy savings, and the products lifetime is essential to confirm the environmental benefits of the proposed strategy.

Declaration of generative AI in scientific writing

The authors declare that they did not use generative AI systems while preparing and writing the manuscript.

CRediT authorship contribution statement

Zaida Ortega: Writing – review & editing, Writing – original draft, Validation, Supervision, Methodology, Investigation, Data curation, Conceptualization. **Paula Douglas:** Writing – review & editing, Investigation, Formal analysis. **Paul R. Hanna:** Writing – review & editing, Investigation. **Jake Kelly-Walley:** Writing – review & editing, Investigation. **Mark McCourt:** Writing – review & editing, Methodology.

Declaration of competing interest

The authors declare that they have no known competing financial interests or personal relationships that could have appeared to influence the work reported in this paper.

Data availability

Data will be made available on request.

Acknowledgments

Plan de Recuperación, Transformación y Resiliencia del Gobierno de España: C21.I4.P1. Resolución del 2 de julio de 2021 de la Universidad de Las Palmas de Gran Canaria por la que se convocan Ayudas para la recualificación del sistema universitario español para 2021–2023.

References

[1] C. Gogos, Z. Tadmor, Principles of Polymer Processing, first ed., John Wiley & Sons, Inc., Canada, 1979.
[2] Roy J. Crawford, Mark P. Kearns, Practical Guide to Rotational Moulding, 2020. http://www.sciencedirect.com:5070/book/9780128224069/practical-guide-to-rotational-moulding. (Accessed 24 January 2023).
[3] Rotomolding Market | Global Industry Report, 2023, (n.d.). https://www.transparencymarketresearch.com/rotomolding-market.html (accessed December 5, 2022).
[4] A. Greco, A. Maffezzoli, S. Forleo, Rotational molding of bio-polymers, in: Proceedings of PPS-29, AIP Conference Proceedings, 2014, pp. 333–337, https://doi.org/10.1063/1.4873794.
[5] K. Ogila, M. Shao, W. Yang, J. Tan, Rotational molding: a review of the models and materials, Express Polym. Lett. 11 (2017) 778–798, https://doi.org/10.3144/expresspolymlett.2017.75.
[6] F.E. Hanana, Y. Chimeni, D. Rodrigue, D. Rodrigue, Morphology and Mechanical Properties of Maple Reinforced LLDPE Produced by Rotational Moulding: Effect of Fibre Content and Surface Treatment, 2018.
[7] C.T. Bellehumeur, M.K. Bisaria, J. Vlachopoulos, An experimental study and model assessment of polymer sintering, Polym. Eng. Sci. 36 (1996) 2198–2207, https://doi.org/10.1002/PEN.10617.
[8] B.I. Chaudhary, E. Takács, J. Vlachopoulos, Processing enhancers for rotational molding of polyethylene, Polym. Eng. Sci. 41 (2001) 1731–1742, https://doi.org/10.1002/PEN.10870.
[9] L. Suárez, Z. Ortega, F. Romero, R. Paz, M.D. Marrero, Influence of giant reed fibers on mechanical, thermal, and disintegration behavior of rotomolded PLA and PE composites, J. Polym. Environ. 30 (2022) 4848–4862, https://doi.org/10.1007/s10924-022-02542-x.
[10] Z. Ortega, F. Romero, R. Paz, L. Suárez, A.N. Benítez, M.D. Marrero, Valorization of invasive plants from macaronesia as filler materials in the production of natural fiber composites by rotational molding, Polymers 13 (2021) 2220, https://doi.org/10.3390/polym13132220.
[11] E.O. Cisneros-López, A.A. Pérez-Fonseca, Y. González-García, D.E. Ramírez-Arreola, R. González-Núñez, D. Rodrigue, J.R. Robledo-Ortíz, Polylactic acid-agave fiber biocomposites produced by rotational molding: a comparative study with compression molding, Adv. Polym. Technol. 37 (2018) 2528–2540, https://doi.org/10.1002/adv.21928.
[12] J. Andrzejewski, A. Krawczak, K. Wesoły, M. Szostak, Rotational molding of biocomposites with addition of buckwheat husk filler. Structure-property correlation assessment for materials based on polyethylene (PE) and poly(lactic acid) PLA, Compos. B Eng. 202 (2020), 108410, https://doi.org/10.1016/j.compositesb.2020.108410.
[13] Z. Ortega, L. Suárez, J. Kelly-Walley, M. McCourt, Mechanical properties of rotomolded parts with abaca fiber: effect of manufacturing with 1, 2 or 3 layers, Composites Theory and Practice 3 (2023) 1–13. https://kompozyty.ptmk.net/pliczki/preprint/202308_zaida-ortega-luis-suarez-jake.pdf.
[14] S. Díaz, Z. Ortega, M. McCourt, M.P. Kearns, A.N. Benítez, Recycling of polymeric fraction of cable waste by rotational moulding, Waste Manag. 76 (2018) 199–206, https://doi.org/10.1016/j.wasman.2018.03.020.
[15] S.P. Cestari, P.J. Martin, P.R. Hanna, M.P. Kearns, L.C. Mendes, B. Millar, Use of virgin/recycled polyethylene blends in rotational moulding, J. Polym. Eng. 41 (2021) 509–516, https://doi.org/10.1515/polyeng-2021-0065.
[16] L. Pick, P.R. Hanna, L. Gorman, Assessment of processibility and properties of raw post-consumer waste polyethylene in the rotational moulding process, J. Polym. Eng. 42 (2022) 374–383, https://doi.org/10.1515/polyeng-2021-0212.
[17] J. Aniśko, M. Barczewski, P. Mietliński, A. Piasecki, J. Szulc, Valorization of disposable polylactide (PLA) cups by rotational molding technology: the influence of pre-processing grinding and thermal treatment, Polym. Test. 107 (2022), 107481, https://doi.org/10.1016/j.polymertesting.2022.107481.
[18] M. Barczewski, A. Hejna, J. Aniśko, J. Andrzejewski, A. Piasecki, O. Mysiukiewicz, M. Bąk, B. Gapiński, Z. Ortega, Rotational molding of polylactide (PLA) composites filled with copper slag as a waste filler from metallurgical industry, Polym. Test. 106 (2022), 107449, https://doi.org/10.1016/j.polymertesting.2021.107449.
[19] M. McCourt, M.P. Kearns, P. Martin, J. Butterfield, A comparison between conventional and robotic rotational moulding machines, in: IMC34 - 34th International Manufacturing ConferenceAt, Sligo Institute of Technology, 2021.
[20] G. Luciano, M. Vignolo, E. Brunengo, R. Utzeri, P. Stagnaro, Study of microwave-active composite materials to improve the polyethylene rotomolding process, Polymers 15 (2023) 1061, https://doi.org/10.3390/polym15051061.
[21] F. Ortega, A. Sova, M.D. Monzón, M.D. Marrero, A.N. Benítez, P. Bertrand, Combination of electroforming and cold gas dynamic spray for fabrication of rotational moulds: feasibility study, Int. J. Adv. Manuf. Technol. 76 (2015) 1243–1251, https://doi.org/10.1007/s00170-014-6331-4.
[22] P. Malnati, New Era for Rotomolding? Innovative technology and equipment offer superior process control and produce better parts with higher repeatability and reproducibility, n.d, www.4spe.org. (Accessed 18 September 2023).

[23] J. Aniśko, M. Barczewski, Uniaxial rotational molding of bio-based low-density polyethylene filled with black tea waste, Materials 16 (2023) 3641, https://doi.org/10.3390/ma16103641.
[24] Z. Ortega, M.D. Monzón, A.N. Benítez, M. Kearns, M. McCourt, P.R. Hornsby, Banana and abaca fiber-reinforced plastic composites obtained by rotational molding process, Mater. Manuf. Process. 28 (2013) 879–883, https://doi.org/10.1080/10426914.2013.792431.
[25] S.S. Abhilash, R. Lal A, D. Lenin Singaravelu, A comparative study of Mechanical, morphological and vibration damping characteristics of wood fiber reinforced LLDPE processed by rotational moulding, Mater. Today Proc. 59 (2022) 510–515, https://doi.org/10.1016/j.matpr.2021.11.559.
[26] A. Hejna, M. Barczewski, J. Andrzejewski, P. Kosmela, A. Piasecki, M. Szostak, T. Kuang, Rotational molding of linear low-density polyethylene composites filled with wheat bran, Polymers 12 (2020) 1004, https://doi.org/10.3390/POLYM12051004.
[27] J. Kelly-Walley, Z. Ortega, M. McCourt, B. Millar, L. Suárez, P. Martin, Mechanical performance of rotationally molded multilayer mLDPE/banana-fiber composites, Materials 16 (2023) 6749, https://doi.org/10.3390/ma16206749.
[28] Z. Ortega, M. McCourt, F. Romero, L. Suárez, E. Cunningham, Recent developments in inorganic composites in rotational molding, Polymers 14 (2022) 5260, https://doi.org/10.3390/POLYM14235260, 14 (2022) 5260.
[29] K. Głogowska, P. Pączkowski, B. Samujło, Study on the properties and structure of rotationally moulded linear low-density polyethylene filled with quartz flour, Materials 15 (2022) 2154, https://doi.org/10.3390/ma15062154.
[30] M. Daryadel, T. Azdast, M. Khatami, M. Moradian, Investigation of tensile properties of polymeric nanocomposite samples in the rotational molding process, Polym. Bull. 78 (2021) 2465–2481, https://doi.org/10.1007/S00289-020-03225-0/FIGURES/17.
[31] J. Aniśko, M. Barczewski, A. Piasecki, K. Skórczewska, J. Szulc, M. Szostak, The relationship between a rotational molding processing procedure and the structure and properties of biobased polyethylene composites filled with expanded vermiculite, Materials 15 (2022) 5903, https://doi.org/10.3390/MA15175903/S1.
[32] M. Barczewski, J. Aniśko, A. Piasecki, K. Biedrzycka, K. Moraczewski, M. Stepczyńska, A. Kloziński, M. Szostak, J. Hahn, The accelerated aging impact on polyurea spray-coated composites filled with basalt fibers, basalt powder, and halloysite nanoclay, Compos. B Eng. 225 (2021), 109286, https://doi.org/10.1016/J.COMPOSITESB.2021.109286.
[33] M. Barczewski, D. Matykiewicz, O. Mysiukiewicz, P. Maciejewski, Evaluation of polypropylene hybrid composites containing glass fiber and basalt powder, J. Polym. Eng. 38 (2018) 281–289, https://doi.org/10.1515/polyeng-2017-0019.
[34] M. Barczewski, O. Mysiukiewicz, K. Lewandowski, D. Nowak, D. Matykiewicz, J. Andrzejewski, K. Skórczewska, A. Piasecki, Effect of basalt powder surface treatments on mechanical and processing properties of polylactide-based composites, Materials 13 (2020) 5436, https://doi.org/10.3390/ma13235436.
[35] M. Barczewski, K. Sałasińska, A. Kloziński, K. Skórczewska, J. Szulc, A. Piasecki, Application of the basalt powder as a filler for polypropylene composites with improved thermo-mechanical stability and reduced flammability, Polym. Eng. Sci. 59 (2019), https://doi.org/10.1002/pen.24962.
[36] L. Lendvai, F. Ronkay, G. Wang, S. Zhang, S. Guo, V. Ahlawat, T. Singh, Development and characterization of composites produced from recycled polyethylene terephthalate and waste marble dust, Polym. Compos. 43 (2022) 3951–3959, https://doi.org/10.1002/pc.26669.
[37] A.S. Rajawat, S. Singh, B. Gangil, L. Ranakoti, S. Sharma, M.R.M. Asyraf, M. R. Razman, Effect of marble dust on the mechanical, morphological, and wear performance of basalt fibre-reinforced epoxy composites for structural applications, Polymers 14 (2022) 1325, https://doi.org/10.3390/POLYM14071325, 14 (2022) 1325.
[38] V. Cárdenes, D. Cabrera-Guillén, S. López-Piñeiro, V.G.R. de Argandoña, A. Rubio-Ordóñez, The historical significance of the welded tuffs from Arucas, canary Islands, Geoheritage 14 (2022) 46, https://doi.org/10.1007/s12371-022-00680-1.
[39] J. Xiong, H. Lin, H. Ding, H. Pei, C. Rong, W. Liao, Investigation on thermal property parameters characteristics of rocks and its influence factors, Nat. Gas. Ind. B 7 (2020) 298–308, https://doi.org/10.1016/j.ngib.2020.04.001.
[40] M. Barczewski, O. Mysiukiewicz, J. Andrzejewski, A. Piasecki, B. Strzemięcka, G. Adamek, The inhibiting effect of basalt powder on crystallization behavior and the structure-property relationship of α-nucleated polypropylene composites, Polym. Test. 103 (2021), 107372, https://doi.org/10.1016/j.polymertesting.2021.107372.
[41] O. Mysiukiewicz, P. Kosmela, M. Barczewski, A. Hejna, Mechanical, thermal and rheological properties of polyethylene-based composites filled with micrometric aluminum powder, Materials 13 (2020) 1242, https://doi.org/10.3390/ma13051242.
[42] S. Aid, A. Eddhahak, S. Khelladi, Z. Ortega, S. Chaabani, A. Tcharkhtchi, On the miscibility of PVDF/PMMA polymer blends: thermodynamics, experimental and numerical investigations, Polym. Test. 73 (2019), https://doi.org/10.1016/j.polymertesting.2018.11.036.
[43] J.P. Correa-Aguirre, F. Luna-Vera, C. Caicedo, B. Vera-Mondragón, M.A. Hidalgo-Salazar, The effects of reprocessing and fiber treatments on the properties of polypropylene-sugarcane bagasse biocomposites, Polymers 12 (2020), https://doi.org/10.3390/POLYM12071440.
[44] S. Mohanty, S.K. Nayak, Short bamboo fiber-reinforced HDPE composites: influence of fiber content and modification on strength of the composite, J. Reinforc. Plast. Compos. 29 (2010) 2199–2210, https://doi.org/10.1177/0731684409345618.
[45] J. Kubát, M. Rigdahl, M. Welander, Characterization of interfacial interactions in high density polyethylene filled with glass spheres using dynamic-mechanical analysis, J. Appl. Polym. Sci. 39 (1990) 1527–1539, https://doi.org/10.1002/app.1990.070390711.
[46] J. Jyoti, B.P. Singh, A.K. Arya, S.R. Dhakate, Dynamic mechanical properties of multiwall carbon nanotube reinforced ABS composites and their correlation with entanglement density, adhesion, reinforcement and C factor, RSC Adv. 6 (2016) 3997–4006, https://doi.org/10.1039/C5RA25561A.
[47] V. Panwar, K. Pal, An optimal reduction technique for rGO/ABS composites having high-end dynamic properties based on Cole-Cole plot, degree of entanglement and C-factor, Compos. B Eng. 114 (2017) 46–57, https://doi.org/10.1016/j.compositesb.2017.01.066.